Available online at www.sciencedirect.com
ScienceDirect
Biomaterials 28 (2007) 2525–2533
Biomaterials
www.elsevier.com/locate/biomaterials

Noninvasive image analysis of 3D construct mineralization in a perfusion bioreactor

Blaise D. Porter[a,*], Angela S.P. Lin[a,b], Alexandra Peister[b], Dietmar Hutmacher[c,d], Robert E. Guldberg[a,b]

[a]*Woodruff School of Mechanical Engineering, Georgia Institute of Technology, Atlanta, GA 30332, USA*
[b]*Institute of Bioengineering and Bioscience, Georgia Institute of Technology, Atlanta, GA 30332, USA*
[c]*Division of Bioengineering, National University of Singapore, Singapore 117576, Singapore*
[d]*Department of Orthopaedic Surgery, Yong Loo Lin School of Medicine National University of Singapore, Singapore 117576, Singapore*

Received 2 October 2006; accepted 1 January 2007
Available online 26 January 2007

Abstract

Although the beneficial effects of perfusion on cell-mediated mineralization have been demonstrated in several studies, the size of the mineralized constructs produced has been limited. The ability to quantify mineralized matrix formation non-invasively within 3D constructs would benefit efforts to optimize bioreactor conditions for scaling-up constructs to clinically relevant dimensions. In this study, we report a micro-CT imaging-based technique to monitor 3D mineralization over time in a perfusion bioreactor and specifically assess mechanisms of construct mineralization by quantifying the number, size, and distribution of mineralized particle formation within constructs varying in thickness from 3 to 9 mm. As expected, mineralized matrix volume and particle number increased with construct thickness. Analyzing multiple concentric volumes inside each construct indicated that a greater proportion of the mineral volume was found within the interior of the perfused constructs. Interestingly, intermediate-sized 6 mm thick constructs were found to have the highest core mineral volume fraction and the largest mineralized particles. Two complementary mechanisms of increasing total mineral volume were observed in the 6 and 9 mm constructs: increasing particle size and increasing the number of mineralized particles, respectively. The rate of mineralized matrix formation in the perfused constructs increased from 0.69 mm^3/week during the first 3 weeks of culture to 1.03 mm^3/week over the final 2 weeks. In contrast, the rate of mineral deposition in the static controls was 0.01 mm^3/week during the first 3 weeks of culture and 0.16 mm^3/week from week 3 to week 5. The ability to monitor overall construct mineralization non-invasively coupled with quantitative analysis of mineralized particle size, number, and distribution offers a powerful tool for elucidating how mineral growth mechanisms are affected by cell type, scaffold material and architecture, or bioreactor flow conditions.

Keywords: Bioreactor; Bone tissue engineering; Image analysis

1. Introduction

Tissue engineering strategies that combine scaffolds with cells capable of osteogenesis or bioactive proteins offer a potential alternative to bone grafting for treatment of large, clinically challenging bone defects. Several studies have demonstrated that delivery of osteoprogenitor cells or osteoblasts significantly improves repair of long bone and cranial defects [1–5]. An important question is whether culturing bone repair constructs *in vitro* to induce progenitor cells to differentiate and produce mineralized extracellular matrix prior to implantation is advantageous. Some studies suggest that pre-mineralization may enhance subsequent mineral formation *in vivo*, but additional work needs to be done to more fully test this hypothesis. Byers recently showed that pre-mineralized constructs grown *in vitro* in static culture enhanced subsequent ectopic mineral formation *in vivo* [6]. However, most of the observed mineral formation was isolated to the periphery

*Corresponding author.
E-mail address: blaise.porter@tissuegrowth.com (B.D. Porter).

0142-9612/$ - see front matter © 2007 Elsevier Ltd. All rights reserved.
doi:10.1016/j.biomaterials.2007.01.013

of the foam-like scaffolds where cell-mediated mineral had accumulated *in vitro*. This shelling effect around 3D constructs in static culture is due to the lack of a nutrient/waste transport *in vitro* [7,8].

Perfusion bioreactor systems have been established in several laboratories to provide enhanced mass transport and thereby improve the development of mineralized constructs *in vitro* [9–16]. Perfusion of osteogenic medium increases the amount of mineralized matrix produced by cells seeded within 3D scaffolds in a flow rate dependent manner [9]. In addition to improving mass transport, fluid flow delivers shear stresses that are well known to modulate cell function [10,17–19]. Perfusion bioreactors, therefore, offer the potential to develop larger, more mineralized constructs for implantation and can also serve as physiologically relevant 3D model systems for studying cell–scaffold interactions *in vitro* as well as to further test novel tissue engineering strategies prior to work in animal preclinical models.

Although the beneficial effects of perfusion on cell-mediated mineralization have been demonstrated in several studies, the size of the mineralized constructs produced has been limited. Clearly, any clinical application of this approach to creating bone graft substitutes would require demonstration that scaling up to clinically relevant dimensions is feasible. Furthermore, the ability to non-invasively quantify mineralized matrix formation within 3D constructs would benefit efforts to optimize bioreactor conditions and in process control of tissue-engineered constructs. In this study, we report a micro-CT imaging-based technique to non-invasively monitor 3D mineralization over time in a perfusion bioreactor and specifically assess mechanisms of construct mineralization by quantifying the number, size, and distribution of mineralized particles formed within constructs varying in thickness from 3 to 6 to 9 mm. We hypothesized that increasing construct thickness would result in a proportional increase in mineralized matrix volume and particle number but would not affect spatial distribution or particle size. We also hypothesized that multiple micro-CT scans would not negatively affect mineral formation and deposition. To test this hypothesis, our previously described perfusion bioreactor system was modified to allow in-process micro-CT imaging [20].

2. Materials and methods

2.1. Axial perfusion bioreactor system

A bioreactor system capable of axially perfusing constructs 6 mm in diameter and up to 10 mm in thickness was designed and manufactured. Machined out of polysulfone, the three-piece bioreactor employs a collet design to prevent the tubing from twisting when the bioreactor is screwed together and sealed. Gas permeable tubing connects each bioreactor to its own medium reservoir, which can hold 18 ml of medium. The assembled system can be steam sterilized before filling with medium and inserting cell-seeded scaffolds. Medium is pumped through the system using a digital modular control peristaltic pump (Masterflex, Cole-Parmer)

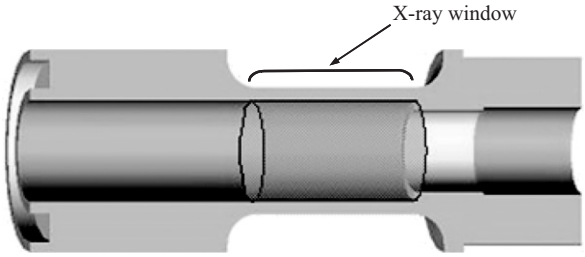

Fig. 1. Perfusion bioreactor capable of being scanned in a micro-CT imaging system. The constructs sit on a small lip to hold them in place. The X-ray window is 10 mm in length.

designed for use in humid environments. To allow for in-process micro-CT imaging, the entire bioreactor chamber was designed to fit into a Viva-CT (Scanco Medical, Bassersdorf, Switzerland) scanner without disconnecting the tubing so that the system remains closed and the constructs sterile. In addition, the bioreactor wall thickness was reduced to 0.76 mm to match the wall thickness of a standard micro-CT sample holder and create an X-ray "window" as shown in Fig. 1.

This perfusion bioreactor system was used for two consecutive studies. In the first, 3 mm thick non-medical grade polycaprolactone (PCL) (Sigma Aldrich) cell-seeded scaffolds were stacked (creating 6 and 9 mm thick scaffolds) to determine the effect of scaffold thickness on mineral deposition. To advance this scaffold technology towards a clinical application, Schantz et al. [21] have used medical grade PCL (mPCL, Birmingham Polymers) as a bone graft substitute for cranioplasty after trephination. In the second experiment, 9 mm thick continuous (non-stacked) mPCL scaffolds (Osteopore LTD, Singapore) were used to test the effect of multiple CT scans on construct mineralization and quantify the effects of perfusion on mineral deposition rate over time in culture.

2.2. Cell harvest

Marrow stromal cells were harvested from 45-day old Sasco Sprague–Dawley rats under guidelines approved by the institutional animal care and use committee. After CO_2 euthanasia, the hind limbs were dissected and soft tissue was aseptically removed. The ends of the femora and tibia were clipped and the marrow was flushed out with medium (α-MEM with 1% antibiotic/antimycotic (a/a), Invitrogen, Carlsbad, CA) using an 18-gauge needle as previously described [22]. Cell aggregates were broken up by trituration using a 10 ml pipette and plated with medium containing 10% FBS and 1% a/a at a density of 75 million cells per 100 mm dish to allow macrophages to adhere. After 45 min, the cell suspension was collected and re-plated at 150 million cells per T-150 flask (Becton Dickinson, Franklin Lakes, NJ). Non-adherent cells were aspirated after 2 days and fresh medium added. The cells were grown until confluence, dissociated from the flask (0.25% trypsin with EDTA, Invitrogen), and frozen in 90% FBS (Hyclone, Logan, UT) and 10% dimethyl sulfoxide (Fisher Scientific) for later use.

2.3. Construct seeding and perfusion culture

Fused deposition modeling was used to fabricate 3 mm thick PCL lattice sheets comprised of 300 μm thick struts spaced 500 μm apart and layered in a 0°/60°/120° repeating pattern to produce an architecture with 66% porosity. Details about the fabrication process can be found elsewhere [23]. Scaffolds were cut from the sheet using a 6 mm biopsy punch (Miltex, York, PA) and then incubated in 5 M NaOH for 12 h at 37 °C for cleaning purposes as well as to partially degrade the scaffold and increase surface roughness. Scaffolds were rinsed twice in one liter of fresh double deionized water under stir bar agitation and then sterilized by 70% EtOH evaporation overnight in a cell culture flow hood. After cleaning and sterilizing the PCL scaffolds, type I rat tail collagen (Vitrogen 100,

Cohesion, Palo Alto, CA) was lyophilized into the pore space, which formed a microporous mesh throughout the polymer (PCL + Col). Briefly, 100 parts collagen (1.4 mg/ml in 0.05% acetic acid) was combined with 9 parts sodium bicarbonate. Seventy-five microliter aliquots of the solution were deposited on each scaffold in order to fill the pore space. Scaffolds were transferred aseptically to 6 well plates and stood at room temperature for 30 min to allow the collagen to gel. The 6 well plates were transferred to a −80 °C freezer for 90 min until the gels were frozen and then placed in a lyophilizer (Labconco, Kansas City, MO) overnight.

Rat marrow stromal cells (rMSCs) were thawed, seeded at 1.5 million cells/150 mm tissue culture dish, expanded for one passage, trypsinized, and seeded on each scaffold. Two million cells suspended in 25 μl of basal medium were deposited on each scaffold and placed in an incubator. After 1 h, 6 ml of medium was added to each well. After 1 week, constructs were stacked on top of each other in each bioreactor to create three experimental groups: 3, 6 and 9 mm thick constructs ($n = 6$). Constructs were axially perfused for 5 weeks with 12 ml of medium for each construct containing osteogenic supplements (50 μg/ml ascorbic acid 2-phosphate, 3 mM β–glycerophosphate, 10 nM dexamethasone) at 0.2 ml/min. Perfusion was stopped for a short period each week to exchange medium within the bioreactor reservoir. Monolayer control cultures were grown alongside each 3-D perfusion experiment. Von Kossa staining after 21 days confirmed that each thawed cell population produced similar amounts of mineralized matrix in 2-D culture (data not shown).

2.4. Micro-CT analysis

After 5 weeks of culture, constructs were carefully removed from each bioreactor and inserted into polycarbonate sleeves for micro-CT analysis. *In vitro* mineralization within perfused constructs was quantified using a Micro-CT 40 scanner (Scanco Medical) at a voxel size of 16 μm. Samples were evaluated at a threshold of 72, a filter width of 1.2 and filter support of 2.0. X-ray attenuation was correlated to sample density using a standard curve generated by scanning hydroxyapatite phantoms with known mineral density. A threshold of 72 correlated to a linear attenuation of 1.15 cm^{-1} and a mineral density of 95 mg HA/cm^3.

Mineralized matrix volume, volume fraction, and density were quantified throughout the entire construct as well as within a cylindrical subregion that excluded the outer 1000 μm of the construct on the top and rounded sides. The two volumes of interest were analyzed to quantify the mineral penetration depth into the construct as well as to determine if the mineral deposition was uniform throughout the construct. Mineral particle size and number were also quantified in this experiment. An image-processing language (IPL) script was used to label the mineral particles and rank them by size. The particle size data did not follow a normal Gaussian distribution; 5% of the total number of particles accounted for over 90% of the detected mineral. In addition to quantifying the total number of particles as a function of scaffold thickness, a subset including only the largest particles that collectively comprised 90% of the total mineral volume was also analyzed. The data were transformed and graphed as a cumulative distribution plot with the percentage of cumulative particles plotted as a function of particle size and graphed on a log scale.

2.5. In-process micro-CT imaging

In-process micro-CT imaging of live 9 mm constructs was used to evaluate the rate of mineralized matrix formation over time and the potential effects of multiple micro-CT exposures. Fused deposition modeling was used to fabricate 9 mm thick PCL lattice sheets comprised of 400 μm thick struts spaced 800 μm apart and layered in a 0°/60°/120° repeating pattern to produce a 75% porous structure. Scaffolds were cut using a 6 mm biopsy punch (Miltex) to create cylindrical scaffolds (6 mm ∅ × 9 mm thick), which were then incubated in 5 M NaOH for 4 h at 37 °C. To standardize the gel fabrication process for these large mPCL scaffolds, 6 mm holes were milled out of a polycarbonate block to create an array of molds. To prevent collagen from leaking out the bottom of the drilled holes, a thin piece of neoprene was compressed between the block and a polycarbonate sheet with screws to plug all the holes. After placing the blocks in polycarbonate boxes, each assembly was autoclaved. Two hundred and twenty-five microliters of the collagen/sodium bicarbonate solution was deposited in each of the holes. Cut scaffolds were then inserted into each sterile mold before the collagen solution polymerized. The collagen solution seeped up through the scaffold and infiltrated the pore space. After replacing the polycarbonate box lids, the molds were then incubated at room temperature for 30 min to allow the collagen to gel. The boxes were transferred to a −80 °C freezer for 90 min until frozen and finally placed in a lyophilizer (Labconco) overnight.

Due to the higher porosity of the mPCL scaffolds, the seeding protocol was modified to accommodate the larger volume available for the cell suspension. Cells were expanded to passage 2 and seeded on mPCL + Col scaffolds (6 mm ∅ × 9 mm thick) at 6 million cells per 120 μl of basal medium. The collagen mesh retained the medium/cell suspension and constructs were subsequently placed in an incubator. After 1 h, 9 ml of medium without osteogenic supplements was added to each well to cover the entire construct. After 3 days in culture, constructs were placed in the bioreactor and perfused at 0.2 ml/min with 18 ml of osteogenic medium or placed in static culture with 18 ml of medium. Ten milliliters of medium with osteogenic supplements was changed once per week, which left 8 ml of conditioned medium in the tubing or the static wells at all times. The static constructs were cultured in custom designed polycarbonate 6 well plates (3.5 cm deep wells) to accommodate 18 ml of medium. After 3 weeks, half of the perfused constructs ($n = 6$) and half of the static constructs ($n = 6$) were scanned in the Viva-CT at a voxel size of 21.5 μm and subsequently returned to perfusion or static culture. At 5 weeks, all scaffolds were scanned at the same spatial resolution. Therefore, one group was scanned only once (5 weeks) and one group was scanned twice (3 and 5 weeks). Mineral volume and density were quantified at both time points. Representative constructs were stained with calcein (green) and ethidium homodimer (red) and imaged with a laser scanning confocal microscope (Zeiss, Germany) to visualize cell viability for both experimental groups at 0 and 5 weeks.

2.6. Fourier transform infrared (FT-IR) spectroscopy

Fourier transform infrared (FT-IR) spectroscopy was used to analyze the chemical composition of the mineralized matrix that was deposited by the rMSCs for all experiments. Samples were prepared as described by Byers [24]. Briefly, cultures were fixed in 70% EtOH and dried in an oven at 40 °C to remove all aqueous components. A scalpel was used to scrape mineral deposits off the PCL scaffold. The mineral was combined with Potassium Bromide (KBr) and compressed between two platens to form a thin film of mineral and KBr. KBr, an ionic salt that cannot be excited by the FT-IR beam, leaves no chemical signature to confound the mineral composition results. Spectra which showed peaks corresponding to chemical bonds, were comprised of 64 scans acquired at 4 cm^{-1} and were collected on a Nexus 470 FT-IR spectrometer (Thermo Nicolet, Madison, WI) under N_2 purge. These spectra were displayed from 400 to 2000 cm^{-1}, which is the range that includes bonds that are characteristic of biological hydroxyapatite.

2.7. Data analysis

Data are reported as mean ± SEM and statistical analyses using Minitab12 were carried out using a general linear model (ANOVA) and Tukey's post-hoc test for pairwise comparisons with $p < 0.05$ considered significant. Regression analysis was also performed in Minitab12. The Kolmogorov–Smirnov test was used to compare the particle size cumulative distribution data sets.

3. Results

3.1. Effect of construct thickness

Visual inspection of all constructs after perfusion revealed significant extracellular matrix deposition, which

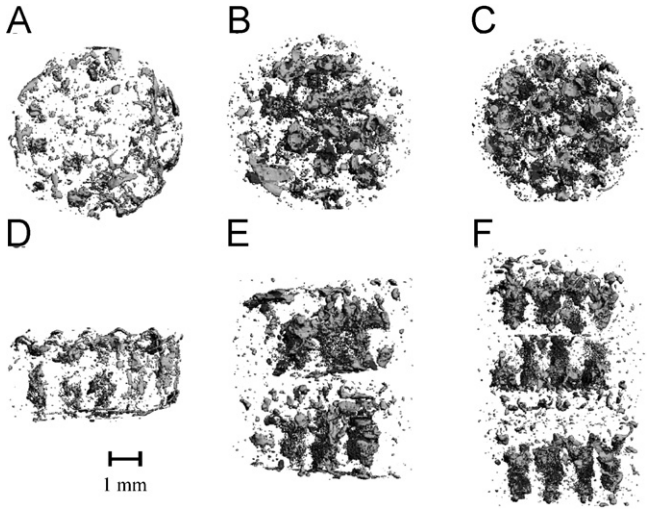

Fig. 2. Representative micro-CT images of mineral deposits within stacked PCL + C scaffolds after 5 weeks of perfusion culture at 0.2 ml/min. Images in the top row (A–C) show the distribution of mineral looking at the constructs from the top. Images in the bottom row (D–F) depict mineral deposits throughout the full thickness of the constructs, which correlate to the images in the top row. The 6 and 9 mm constructs (E, F) show mineral localized within each individual 3 mm thick scaffold, but few mineral deposits at the interfaces between each scaffold.

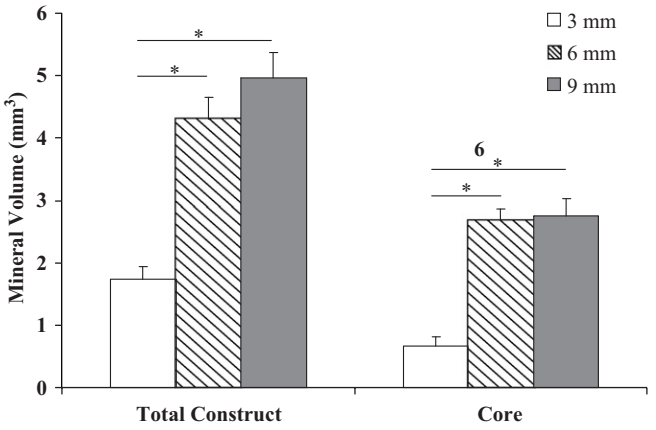

Fig. 3. Mineralized matrix volume for perfused constructs of three different stacked thicknesses ($n = 6$/group) after 5 weeks of perfusion culture at 0.2 ml/min. Two different volumes of interest were analyzed for each construct: (1) total construct, (2) a cylindrical subregion that excluded the outer 500 μm on the top surface and the outer 1000 μm on the rounded outer surface (core). General Linear Model analysis (ANOVA) showed significant differences between mineral volumes detected in each construct size ($p < 0.001$). Pair wise comparisons of the total construct (*, $p < 0.0002$) revealed a significant increase in mineralized matrix formation within the 6 and 9 mm constructs (4.31 and 4.97 mm^3) compared with the 3 mm thick constructs (1.74 mm^3). The same effect was shown in core subregion as well. There was not a significant increase in mineral volume when the length was further increased from 6 to 9 mm for either evaluation region.

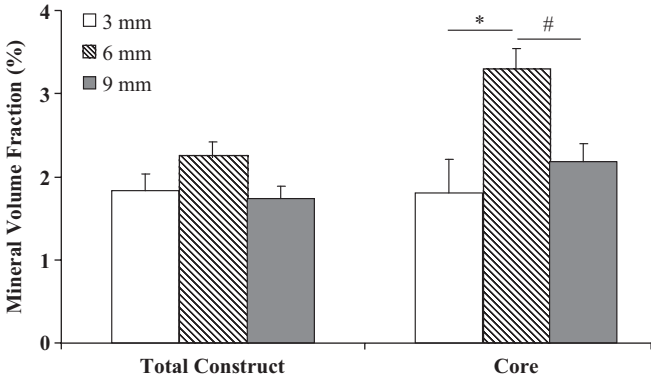

Fig. 4. Mineralized matrix volume fraction (MVF) for perfused constructs of three different stacked thicknesses ($n = 6$/group) after 5 weeks of perfusion culture at 0.2 ml/min. Mineral volumes from Fig. 3 were normalized by the volume of region analyzed. General linear model ANOVA showed differences in groups ($p < 0.0001$). There were no significant differences in MVF when comparing mineral within the total volume of each construct. Pair wise comparisons showed a significant increase in MVF for the 6 mm constructs compared to the 3 mm constructs (*, $p < 0.0053$). There was also a trend towards a significant increase in MVF for the 6 mm constructs over the 9 mm constructs (#, $p < 0.0867$).

entirely filled the majority of the pores. Micro-CT images displayed mineral deposition throughout the entire thickness of all constructs with no apparent differences between the upstream and downstream ends (Fig. 2). However, reduced mineralized matrix deposition was observed at the interfaces between the stacked 6 and 9 mm constructs.

The total detected mineral volume increased 2.85-fold as the construct thickness was increased from 3 to 9 mm, while a 2.5-fold increase was detected in the 6 mm constructs compared with the 3 mm constructs (Fig. 3). There was no statistical difference between the amount of mineral detected in the 6 and 9 mm constructs. Isolating the analysis region to the interior core of the constructs revealed a 4-fold higher mineralized matrix volume for both the 6 and 9 mm constructs compared with the 3 mm constructs. When normalized by pore volume, there were no statistical differences in the mineral volume fraction (MVF) across any of the construct sizes when analyzing the entire construct volume (Fig. 4). However, the 6 mm constructs had a higher core MVF compared to the 3 mm ($p < 0.01$) and 9 mm ($p = 0.087$) constructs.

The uniformity of the mineral distribution for each scaffold type is displayed in Fig. 5 by plotting the percentage of total mineral observed within increasingly larger volumes of interest from the center outward. The dotted straight line represents an idealized construct with a uniform radial distribution of mineral. A line for constructs grown in static culture, which form a mineralized exterior shell would fall below the idealized line (data not shown). In contrast, the distribution lines for all of the perfused constructs were above the idealized line, indicating that a greater proportion of the mineral volume was found within the interior of the constructs. This non-uniformity was more evident in the 6 and 9 mm constructs than the 3 mm constructs.

The mean values of mineral density expressed in mg HA/cm^3 within the entire construct and the interior core subregion were determined for each construct size

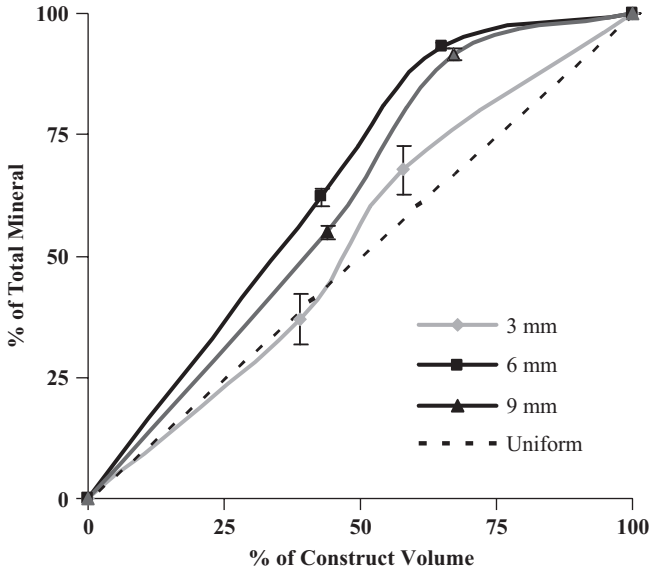

Fig. 5. Mineral distribution within perfused constructs of three different stacked thicknesses ($n = 6$/group). Plot of the percentage of the total mineral detected in each evaluation subregion. An ideal construct with perfectly uniform mineral distribution throughout the scaffold would follow the dashed line. All three groups show a concentration of mineral deposition at the construct interior with the greatest non-uniformity observed in the thicker constructs.

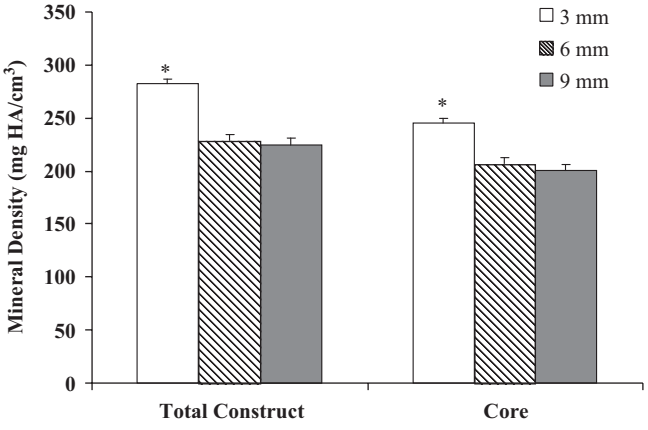

Fig. 6. Mineralized matrix density measured by micro-CT for constructs of three different stacked thicknesses ($n = 6$/group) perfused at 0.2 ml/min. Mineral attenuation was correlated to a standard curve generated by scanning hydroxyapatite phantoms with known mineral density. General Linear Model ANOVA showed significant differences among the densities of the mineralized matrix detected in the different construct groups (*, $p < 0.001$). Pair wise comparisons showed that the mineral density detected in the 6 and 9 mm thick constructs was significantly lower than the density of the mineral in the 3 mm thick constructs for both analysis regions.

(Fig. 6). Regardless of region analyzed, the mineral density detected in the 3 mm thick constructs was significantly higher (~25%) than the density of the mineral in the 6 and 9 mm thick constructs.

The number and size of mineral particles within the PCL + Col constructs was significantly affected by construct thickness. Regression analysis indicated the total number of mineralized particles increased linearly with construct size ($R^2 = 92.9\%$, Fig. 7). There was a 74% increase in the number of particles detected in the 6 mm constructs compared with the 3 mm constructs, and a 78% increase in the number of particles detected in the 9 mm constructs compared with the 6 mm constructs. For all constructs, regardless of thickness, over 90% of the total mineral volume was accounted for by less than 5% of the total number of particles. The very large number of tiny particles produced a highly skewed distribution of particle sizes. Therefore, a cumulative distribution plot of the largest particles representing 90% of the mineral volume was generated to analyze differences in particle size as a function of construct thickness. The Kolmogorov–Smirnov test, which allows for non-normal data distributions, was used to test for differences between the groups. Significant differences were found between all three groups; the largest mineralized particles were found in the 6 mm constructs followed by the 9 mm and then the 3 mm constructs (Fig. 8).

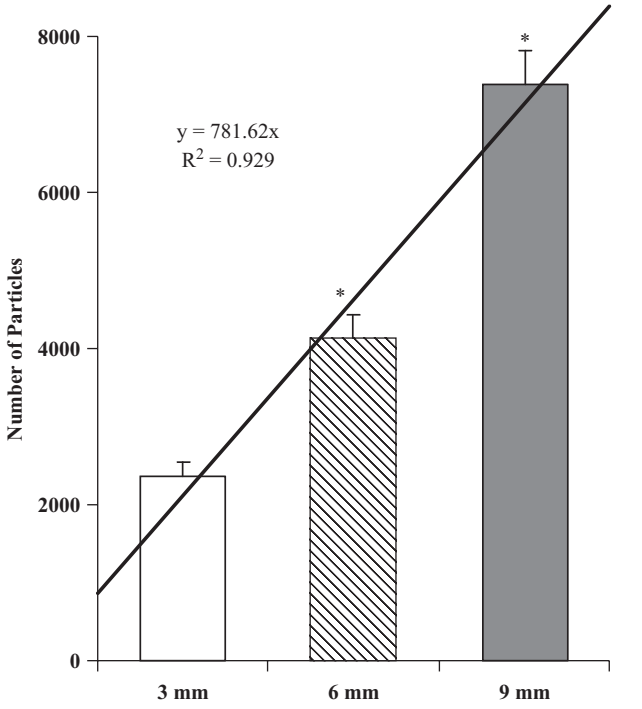

Fig. 7. Plot of the total number of mineral particles for each stacked construct thickness ($n = 6$/group). Pair wise comparisons indicated a statistically significant difference in the number of mineral particles detected for each different construct thickness. Regression analysis in Minitab indicated that the increase in the number of particles as a function of construct length followed a linear trend ($R^2 = 0.929$).

To confirm that mineralization within the perfused constructs was biological, FT-IR spectroscopy was used to characterize the chemical composition of the mineralized matrix deposited by rMSCs. The observed spectra in Fig. 9 displayed peaks that are representative of physiological bone composition [25]. Mineral from all three construct

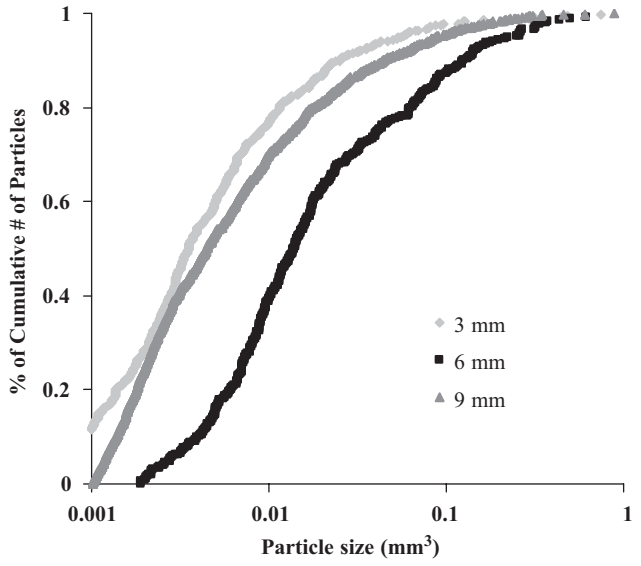

Fig. 8. Cumulative distribution plots illustrating the distribution of mineral particle sizes after 5 weeks in culture for each size construct. The Kolmogorov–Smirnov test determined that all the distributions were statistically different. The particles in the 6 mm constructs were significantly larger than those in both the 3 and 9 mm constructs. The particles in the 9 mm constructs were significantly larger than the particles in the 3 mm constructs ($p<0.001$ for all comparisons).

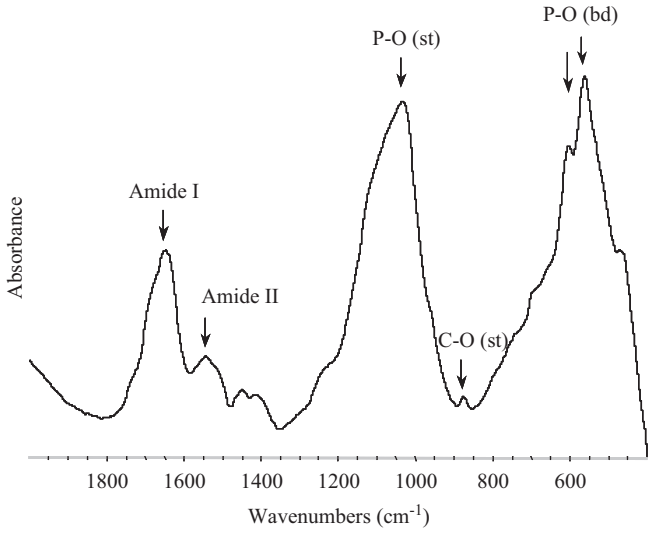

Fig. 9. Representative FT-IR spectrum of mineral deposits removed from a 6 mm stacked PCL + Col construct. Mineral from all three scaffold lengths exhibited the amide I and II peaks which correlate to protein. The stretching (st) phosphate peaks near 1100 cm^{-1}, the stretching (st) carbonate peak at 870 cm^{-1} as well as the phosphate bending (bd) doublet at 605 and 560 cm^{-1} were also apparent in the mineral from all three thicknesses. The above spectrum is characteristic of biological hydroxyapatite.

thicknesses exhibited the amide I and II peaks at 1650 and 1540 cm^{-1} which correlate to protein. The stretching (st) phosphate peaks near 1100 cm^{-1}, the stretching (st) carbonate peak at 870 cm^{-1}, as well as the phosphate bending (bd) doublet at 605 and 560 cm^{-1} were also apparent in the mineral from all three groups of constructs.

3.2. Rate of mineralization and effect of repeat scanning

Confocal microscopy showed a majority of live cells distributed throughout perfused constructs with no discernable difference between contructs scanned twice versus those only scanned at 5 weeks. Consistent with our previous studies, constructs grown in static culture contained fewer live cells and more dead cells than perfused constructs, particularly at the center of the constructs.

3D images of mineral deposition on mPCL + Col constructs revealed mineral deposition throughout the entire thickness of perfused 9 mm thick constructs, whereas only trace amounts of mineral were present in the static constructs at both 3 and 5 weeks (Fig. 10). No significant differences were detected in mineralized matrix volume within perfused constructs that had been scanned twice compared to those that had been scanned once (Fig. 11). In-process scanning also had no effect on the density of mineralized matrix formation, however, perfusion resulted in a small but statistically significant increase in density compared to static controls by 5 weeks of culture (data not shown). The rate of mineralized matrix formation in the perfused constructs increased from 0.69 mm^3/week during the first 3 weeks of culture to 1.03 mm^3/week from week 3 to week 5. In contrast, the rate of mineral deposition in the static controls was 0.01 mm^3/week during the first 3 weeks of culture and 0.16 mm^3/week from week 3 to week 5 (Fig. 12). Additionally, there were no significant differences in mineral density for scaffolds that had been scanned twice compared to those that had been scanned once (data not shown).

4. Discussion

Bioreactor systems that enhance mass transport and deliver controlled mechanical stimuli have been shown to improve extracellular matrix synthesis *in vitro* and may offer the ability to produce tissue constructs of clinically relevant size and shape [26]. In this study, we tested the effects of increasing scaffold thickness on the number, size, and distribution of mineralized particles deposited within PCL + Col scaffolds seeded with marrow stromal cells and perfused with osteogenic medium. The second objective of this study was to establish a micro-CT based method to provide in-process quantification of mineralized matrix formation and use this approach to assess the rate of construct mineralization over time. This work lays a foundation for future studies evaluating cell-scaffold interactions and optimizing bioreactor conditions *in vitro* as well as testing functional integration of large mineralized constructs *in vivo*.

Micro-CT analysis of perfused constructs revealed mineralized matrix formation throughout the thickness of all constructs, suggesting that it should be possible to

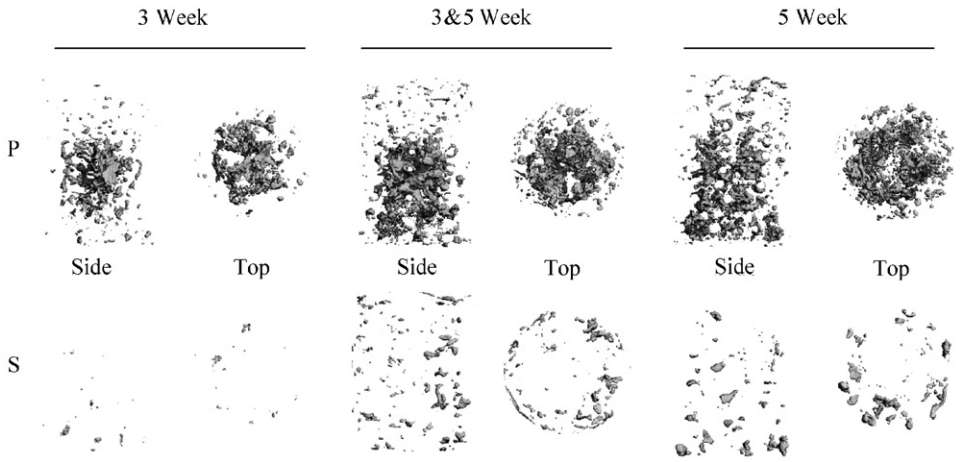

Fig. 10. Representative Viva-CT images of perfused (row P) and statically (row S) cultured mPCL + Col 9 mm continuous scaffolds seeded with rMSCs. To evaluate the effects of in-process micro-CT scanning, constructs were either scanned at 3 and 5 weeks or 5 weeks only.

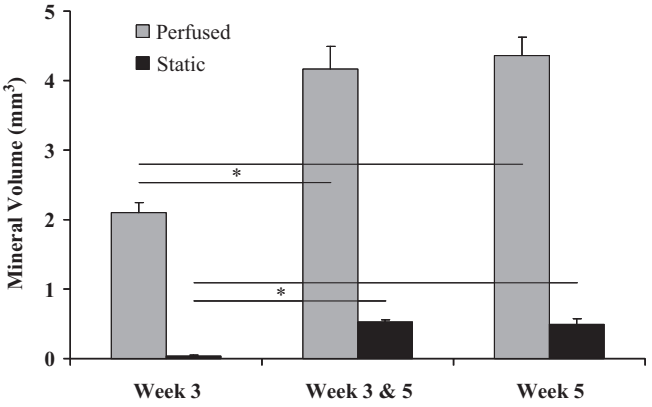

Fig. 11. Mineralized matrix volume within continuous 9 mm thick 75% porous mPCL + Col constructs ($n = 8$) detected by micro-CT scanning at a voxel resolution of 21.5 μm. One group of constructs was scanned at 3 and 5 weeks while the second group was scanned only at 5 weeks. General Linear Model ANOVA showed no significant differences in mineralized matrix volume within constructs that had been scanned twice compared with those that had been scanned once ($p = 0.8606$). Constructs in static culture produced significantly less mineral than perfused constructs at both time points ($p < 0.001$). Mineral volume increased in both perfused and static groups with time in culture from 3 to 5 weeks ($p < 0.0002$).

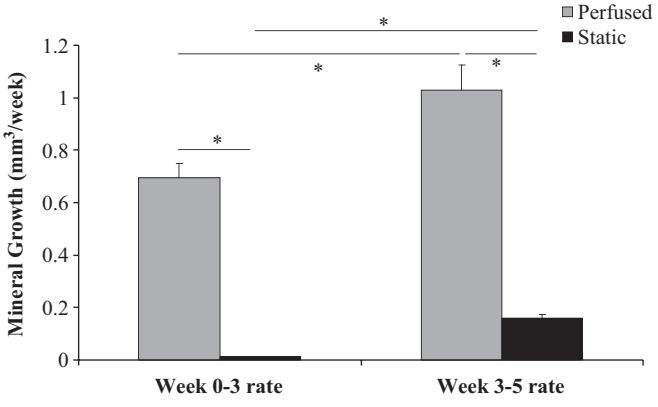

Fig. 12. Mineral growth rate between 0–3 weeks and 3–5 weeks for perfused and static continuous 9 mm thick mPCL-Col constructs. The growth rate for perfused constructs between week 0 and 3 was over 50-fold greater than the growth rate for static constructs (*, $p < 0.05$) during the same time. The growth rate between weeks 3 and 5 for perfused constructs was 6.5 times greater than static constructs. There was a 49% increase in mineral growth rate for perfused constructs between 0–3 and 3–5 weeks.

produce constructs larger than 9 mm in thickness in perfusion culture. As shown in Fig. 5, mineralization was greater at the core of perfused constructs than on the periphery, regardless of construct thickness. This spatial distribution of mineral deposition is essentially the inverse of that observed within constructs grown in static culture [8,27]. The reduced mineralization around the periphery of perfused constructs may be due to the small lip in the bioreactor wall used to retain the construct in a fixed position. That lip directs medium to the central annulus of the construct.

The design and composition of the mPCL + Col scaffolds used for these studies was also likely an important factor affecting the uniformity of media perfusion and distribution of mineralization. Fused deposition fabrication provided a macroporous PCL scaffold having a channel-like architecture with large pore interconnections. We have previously shown that media perfusion through scaffolds with more complex pore structures can be highly non-uniform [20]. The addition of lyophilized collagen to the PCL scaffolds was intended to improve the seeding efficiency and retention of cells under perfusion. The composite scaffold design also encouraged matrix deposition across the large pores (>500 μm) and not just on the PCL strut surfaces. Although not entirely mineralized, gross observation by the naked eye revealed that extracellular matrix appeared to completely fill most of the pores at the ends of the constructs, and mineralized

particles were formed throughout the pores within the construct interior. Interestingly, mineralization was reduced at the interfaces between stacked 3 mm constructs. This may have been due to discontinuity of pores or a lack of collagen between adjacent constructs. Supporting this interpretation, the axial non-uniformity observed in the stacked constructs was not seen in the subsequent multiple scan study that used intact 9 mm constructs.

Although mineral distribution was not strongly affected by construct thickness, differences in mineral density, volume, and volume fraction as well as particle size and number were observed. As expected, the number and total volume of mineralized particles increased with increasing construct thickness. However, the difference in mineral volume between the 6 mm and 9 mm constructs was not significant. Furthermore, the core MVF in 6 mm constructs was significantly higher than that measured for 3 and 9 mm constructs. This difference was at least in part explained by a significantly higher mineral particle size in the 6 mm constructs. The larger particles in the 6 mm constructs may have resulted from growth of individual nucleation sites or conjunction of several particles that grew together. In contrast, the 9 mm constructs had a larger number of smaller particles, resulting in a similar overall volume of mineralized matrix. Interestingly, the 3 mm constructs had the highest mineral density. This may suggest that the thicker constructs contained more newly formed particles; however, longer-term studies that allow the system to reach equilibrium would be needed to confirm this supposition.

The second set of experiments demonstrated that neither mineral volume nor density measured within intact perfused 9 mm constructs at 5 weeks were affected by in-process micro-CT scanning of the constructs at 3 weeks. This result is consistent with our previous static culture study in which weekly micro-CT scans did not significantly alter cell-mediated construct mineralization [8]. Calculations of mineralization rates made possible by micro-CT analysis of constructs within their bioreactors indicated that construct mineralization rate was higher in perfused constructs compared to static controls and increased with time in culture for both experimental groups. The described image-based analysis method may be beneficial for optimization of bioreactor conditions such as flow rate and is complementary to other recently reported methods of monitoring mineralized construct development such as measurement of oxygen consumption [14]. Such methods combined with this novel perfusion bioreactor may also be useful for efficiently evaluating different flow rates on MSC differentiation as well as cell–scaffold interactions to improve bone tissue-engineering strategies in a well controlled *in vitro* environment.

5. Conclusion

An imaging method using micro-CT scanning and a transportable perfusion bioreactor system was developed to aseptically quantify and analyze mineral formation over time in culture within cell-seeded scaffolds. This study demonstrated for the first time that constructs measuring up to 9 mm in thickness and having mineralized matrix throughout may be generated *in vitro*. Using macroporous scaffolds with a uniform pore morphology combined with lyophilized collagen, it is likely that even larger mineralized constructs can be engineered. Even so, the observation that the intermediate-sized 6 mm constructs produced the largest particles and core MVF suggests there may be a limit to the size of constructs that can be produced by this approach. Two complementary mechanisms of increasing total mineral volume were observed in the 6 and 9 mm constructs: increasing particle size and increasing the number of mineralized particles, respectively. The ability to non-invasively monitor overall construct mineralization coupled with quantitative analysis of mineralized particle size, number, and distribution offers a powerful tool for elucidating how mineral growth mechanisms are affected by cell type, scaffold design, or bioreactor conditions.

Acknowledgments

This work was supported by the Georgia Tech/Emory Center for the Engineering of Living Tissues (GTEC) NSF Grant EEC-9731643, NIH Grant AR051336, and NIH Grant No. 5K12GM000680-07.

References

[1] Schantz JT, Hutmacher DW, Lam CX, Brinkmann M, Wong KM, Lim TC, et al. Repair of calvarial defects with customised tissue-engineered bone grafts II. Evaluation of cellular efficiency and efficacy in vivo. Tissue Eng 2003;9(Suppl. 1):S127–39.

[2] Bruder SP, Fox BS. Tissue engineering of bone. Cell based strategies. Clin Orthop Relat Res 1999(Suppl. 367):S68–83.

[3] Lane JM, Yasko AW, Tomin E, Cole BJ, Waller S, Browne M, et al. Bone marrow and recombinant human bone morphogenetic protein-2 in osseous repair. Clin Orthop Relat Res 1999(361): 216–27.

[4] Einhorn TA. Clinically applied models of bone regeneration in tissue engineering research. Clin Orthop 1999(Suppl. 367):S59–67.

[5] Brodke D, Pedrozo HA, Kapur TA, Attawia M, Kraus KH, Holy CE, et al. Bone grafts prepared with selective cell retention technology heal canine segmental defects as effectively as autograft. J Orthop Res 2006;24(5):857–66.

[6] Byers BA, Guldberg RE, Garcia AJ. Synergy between genetic and tissue engineering: Runx2 overexpression and in vitro construct development enhance in vivo mineralization. Tissue Eng 2004; 10(11–12):1757–66.

[7] Ishaug-Riley SL, Crane-Kruger GM, Yaszemski MJ, Mikos AG. Three-dimensional culture of rat calvarial osteoblasts in porous biodegradable polymers. Biomaterials 1998;19(15):1405–12.

[8] Cartmell S, Huynh K, Lin A, Nagaraja S, Guldberg R. Quantitative microcomputed tomography analysis of mineralization within three-dimensional scaffolds in vitro. J Biomed Mater Res 2004;69A(1): 97–104.

[9] Bancroft GN, Sikavitsas VI, van den Dolder J, Sheffield TL, Ambrose CG, Jansen JA, et al. Fluid flow increases mineralized matrix deposition in 3D perfusion culture of marrow stromal osteoblasts in a dose-dependent manner. Proc Natl Acad Sci USA 2002;99(20):12600–5.

[10] Cartmell SH, Porter BD, Garcia AJ, Guldberg RE. Effects of medium perfusion rate on cell-seeded three-dimensional bone constructs in vitro. Tissue Eng 2003;9(6):1197–203.
[11] Glowacki J, Mizuno S, Greenberger JS. Perfusion enhances functions of bone marrow stromal cells in three-dimensional culture. Cell Transplant 1998;7(3):319–26.
[12] Goldstein AS, Juarez TM, Helmke CD, Gustin MC, Mikos AG. Effect of convection on osteoblastic cell growth and function in biodegradable polymer foam scaffolds. Biomaterials 2001;22(11): 1279–88.
[13] Holtorf HL, Jansen JA, Mikos AG. Flow perfusion culture induces the osteoblastic differentiation of marrow stroma cell–scaffold constructs in the absence of dexamethasone. J Biomed Mater Res A 2005;72(3):326–34.
[14] Janssen FW, Oostra J, Oorschot A, van Blitterswijk CA. A perfusion bioreactor system capable of producing clinically relevant volumes of tissue-engineered bone: in vivo bone formation showing proof of concept. Biomaterials 2006;27(3):315–23.
[15] Meinel L, Karageorgiou V, Fajardo R, Snyder B, Shinde-Patil V, Zichner L, et al. Bone tissue engineering using human mesenchymal stem cells: effects of scaffold material and medium flow. Ann Biomed Eng 2004;32(1):112–22.
[16] Braccini A, Wendt D, Jaquiery C, Jakob M, Heberer M, Kenins L, et al. Three-dimensional perfusion culture of human bone marrow cells and generation of osteoinductive grafts. Stem Cells 2005;23(8): 1066–72.
[17] Sikavitsas VI, Bancroft GN, Holtorf HL, Jansen JA, Mikos AG. Mineralized matrix deposition by marrow stromal osteoblasts in 3D perfusion culture increases with increasing fluid shear forces. Proc Natl Acad Sci USA 2003;100(25):14683–8.
[18] Klein-Nulend J, Helfrich MH, Sterck JG, MacPherson H, Joldersma M, Ralston SH, et al. Nitric oxide response to shear stress by human bone cell cultures is endothelial nitric oxide synthase dependent. Biochem Biophys Res Commun 1998;250(1):108–14.
[19] McAllister TN, Du T, Frangos JA. Fluid shear stress stimulates prostaglandin and nitric oxide release in bone marrow-derived preosteoclast-like cells. Biochem Biophys Res Commun 2000;270(2): 643–8.
[20] Porter B, Zauel R, Stockman H, Guldberg R, Fyhrie D. 3-D computational modeling of media flow through scaffolds in a perfusion bioreactor. J Biomech 2005;38(3):543–9.
[21] Schantz JT, Lim TC, Ning C, Teoh SH, Tan KC, Wang SC, et al. Cranioplasty after trephination using a novel biodegradable burr hole cover: technical case report. Neurosurgery 2006;58(Suppl. 1) ONS-E176; discussion ONS-E176.
[22] Aubin JE. Osteoprogenitor cell frequency in rat bone marrow stromal populations: role for heterotypic cell–cell interactions in osteoblast differentiation. J Cell Biochem 1999;72(3):396–410.
[23] Hutmacher DW, Schantz T, Zein I, Ng KW, Teoh SH, Tan KC. Mechanical properties and cell cultural response of polycaprolactone scaffolds designed and fabricated via fused deposition modeling. J Biomed Mater Res 2001;55(2):203–16.
[24] Byers BA, Garcia AJ. Exogenous Runx2 expression enhances in vitro osteoblastic differentiation and mineralization in primary bone marrow stromal cells. Tissue Eng 2004;10(11–12):1623–32.
[25] Bonewald LF, Harris SE, Rosser J, Dallas MR, Dallas SL, Camacho NP, et al. von Kossa staining alone is not sufficient to confirm that mineralization in vitro represents bone formation. Calcif Tissue Int 2003;72(5):537–47.
[26] Martin I, Wendt D, Heberer M. The role of bioreactors in tissue engineering. Trends Biotechnol 2004;22(2):80–6.
[27] Ishaug SL, Crane GM, Miller MJ, Yasko AW, Yaszemski MJ, Mikos AG. Bone formation by three-dimensional stromal osteoblast culture in biodegradable polymer scaffolds. J Biomed Mater Res 1997;36(1):17–28.